Journal of Hepatocellular Carcinoma

Dovepress
Taylor & Francis Group

Open Access Full Text Article

ORIGINAL RESEARCH

Exploration of the Mechanism of Action of *Dendrobium officinale* in the Treatment of Liver Cancer Based on Network Pharmacology, Molecular Docking and in vitro Validation

Shuimeng Zhan[1,*], Xinyan Lu[1,*], Hongyan Guo[1], Yang Liu[1], Zhi Li[1], Wei Xu[2], Fang Xia[2], Huanjun Tang[2], Yi Tian[2], Jing Chen[3], Xuan Lin[1]

[1]Department of Endocrinology, CR & WISCO General Hospital Affiliated to Wuhan University of Science and Technology, Wuhan, Hubei, People's Republic of China; [2]School of Medicine, Wuhan University of Science and Technology, Wuhan, Hubei, People's Republic of China; [3]Pediatric Department, Dawu County Traditional Chinese Medicine Hospital, Xiaogan, Hubei, People's Republic of China

*These authors contributed equally to this work

Correspondence: Jing Chen; Xuan Lin, Email 490998572@qq.com; 854964946@qq.com

Video Abstract

Point your SmartPhone at the code above. If you have a QR code reader the video abstract will appear. Or use: https://youtu.be/YDI5W2cWrpM

Purpose: The anti-tumor effects of *Dendrobium officinale*, as a medicinal and dietary Chinese medicine, have long been documented. However, the mechanism of action for its therapeutic effect has not been fully elucidated.

Methods: The chemical constituents of *Dendrobium officinale* were screened using PubMed, CNKI, and Wanfang databases. Swiss Target Prediction was used to predict ingredient targets, while liver cancer targets were obtained from multiple databases. Venny 2.1.0 software identified intersection genes between the drug and disease, and a Protein–Protein Interaction (PPI) network was constructed. The DAVID database was used for Gene Ontology (GO) and Kyoto Encyclopedia of Genes and Genomes (KEGG) pathway enrichment analysis. Following this, the compound molecules were docked onto the core targets, and a visual analysis was conducted. The network pharmacology results were experimentally validated through in vitro studies with HepG2 cells.

Results: The study identified 17 core components and 374 ingredient targets, with 1,249 disease targets collected from databases, yielding 50 overlapping targets. GO analysis revealed 284 Biological Process (BP) terms, 38 Cellular Component (CC) terms, and 75 Molecular Function (MF) terms. KEGG enrichment highlighted key pathways, including Pathways in cancer, PI3K-AKT signaling, Prostate cancer, and Proteoglycans in cancer. Molecular docking showed strong activity of Butin, Skimmin, and N-p-Coumaroyltyramine with core targets AKT1, EGFR, and CCND1. In vitro experiments demonstrated that *Dendrobium officinale* aqueous extracts significantly inhibited HepG2 cell proliferation. Western blotting analysis further revealed that the extracts down-regulated the expression levels of p-PI3K, PI3K, AKT1, EGFR, and CCND1 proteins.

Conclusion: The key active components of *Dendrobium officinale* in treating liver cancer include butin, skimmin, and N-p-coumaroyltyramine, etc. The specific mechanism of action may be related to the modulation of targets such as p-PI3K/PI3K, AKT1, EGFR, and CCND1, and signaling pathways such as PI3K-Akt.

Keywords: *Dendrobium officinale*, liver cancer, network pharmacology, molecular docking, in vitro experiments

Introduction

Primary liver cancer (PLC) primarily encompasses three distinct pathological types: hepatocellular carcinoma (HCC), intrahepatic cholangiocarcinoma (ICC), and combined hepatocellular-cholangiocarcinoma (CHC). Among these, HCC accounts for 75–85% of cases, while ICC comprises 10–15%.[1,2] HCC is one of the most severe malignant tumors globally, known as the "king of cancers".[3] The incidence of PLC in China is significantly higher than that of other countries worldwide, accounting for over 40% of global liver cancer cases posing a substantial threat to national health security.[4,5] Epidemiologic

Received: 20 March 2025
Accepted: 10 August 2025
Published: 28 August 2025

studies reveal distinct age distribution characteristics of PLC,[6] with a median diagnostic age of 62 years. However, clinical observations indicate that approximately 14.7% of cases occur in younger populations aged 15–49 years,[7] demonstrating that PLC is not exclusively prevalent among elderly populations. Notably, despite continuous advancements in diagnostic and therapeutic technologies, the clinical prognosis of PLC remains suboptimal, with an overall 5-year survival rate below 20%,[8] which unequivocally confirms the highly aggressive biological nature of this malignancy. The pathogenesis of PLC is multifactorial, involving various established risk factors including viral hepatitis, alcoholic liver disease, non-alcoholic fatty liver disease, diabetes mellitus, obesity, metabolic syndrome, and chronic exposure to certain chemical carcinogens.[9,10] In China, the primary cause of liver cancer is hepatitis B virus infection, which gradually progresses into liver cancer over time. Early-stage patients often exhibit non-obvious symptoms, and symptoms usually manifest in the middle to late stages of the disease. Therefore, the prevention of liver cancer is extremely important.[11] The pathogenesis of liver cancer is associated with aberrant activation of multiple complex signaling pathways, including PI3K/AKT/mTOR, RAS/MAPK, and JAK/STAT pathways.[12,13] Currently, the main treatments for liver cancer include surgical resection, radiotherapy, and chemotherapy.[14] Surgical resection is only suitable for a small proportion of patients with early-stage liver cancer, and chemotherapy drugs carry certain toxic and side effects as well as drug tolerance issues. Therefore, it is of great significance to explore the mechanism of action against liver cancer development by utilizing the active health nutritional diet *Dendrobium officinale* extract. In recent years, traditional Chinese medicine for cancer prevention and treatment has become a new indispensable idea for liver cancer treatment in most Asian countries. *Dendrobium officinale*, as a kind of medicinal and dietary substance, is characterized by high safety, high efficiency and low toxicity, and it can enhance immunity and improve the quality of patient's survival, which can be applied in the whole clinical treatment process, and it highlights a great potential for the treatment of liver cancer.[15]

Dendrobium officinale, also known as Iron Skin Dendrobium, bears the reputation of being the "Plant Gold".[16] It has a sweet and slightly cold nature, with the efficacy of nourishing Yin and dissipating heat.[17] In China, it mainly grows in cool and moist environments with good air circulation and no direct sunlight in southern regions, thriving year-round on cliffs at altitudes above 1000 meters. *Dendrobium officinale*, as a medicinal and edible substance, contains abundant bioactive components. Flavonoids, polyphenols, polysaccharides, and alkaloids serve as its primary active constituents, demonstrating antitumor, antioxidant, hepatoprotective, and choleretic effects.[18,19] It has been demonstrated that the alkaloid components in *Dendrobium officinale* can bring the proliferation of tumor cells under control, mainly by reducing the expression of cell cycle protein-dependent kinases, thus inhibiting the expression of protein-dependent kinases and inhibiting the proliferation of cancer cells.[20] Experiments conducted by Wang et al showed that *Dendrobium officinale* polysaccharides can promote the M1 polarization of tumor-associated macrophages (TAMs) by targeting Toll-like receptor 2(TLR2), thus inhibiting the growth of mouse hepatocellular carcinoma cells (Hepa1-6).[21] Hong and others showed that Erianin, an extract of *Dendrobium officinale*, was used to treat HepG2 cells and normal hepatic LO2 cells, respectively, for a period of time, and it was found that Erianin could significantly reduce the cell survival rate of HepG2 cells.[22] Yang et al cultured SMMC-7721 and HepG2 cells and treated them with Dendrobium extract. They discovered that erianin inhibited HCC proliferation, migration, and invasion while inducing apoptosis through the PI3K-Akt, p38, and ERK signaling pathways, demonstrating erianin's potential as a promising therapeutic agent for HCC.[23] In a separate study, Xing et al established a HepG2 cell model and employed MTT assay and Western blotting to evaluate the anti-cancer effects of polysaccharides isolated from *Dendrobium officinale* stems. Their results revealed that Dendrobium polysaccharides suppressed HepG2 cell proliferation by downregulating Bcl-2 expression and upregulating Bax expression levels.[24] In summary, finding effective anti-liver cancer drugs from the perspective of Chinese medicine has become a viewpoint recognized by the majority of medical experts.

Previous research directions have mostly focused on the extraction of ingredients and pharmacological effects of *Dendrobium officinale*, lacking insights into the mechanisms of action on specific diseases, which has limited breakthroughs and explorations in the clinical treatment of neoplastic diseases. However, network pharmacology integrates multiple research domains including genomics, proteomics, bioinformatics, and pharmacology.[25] It emphasizes a systems-level approach to elucidate the holistic relationships between the multi-component, multi-target, and multi-pathway characteristics of Chinese herbal medicine and disease targets from the perspective of biological network integrity.[26] For instance, Fang et al employed network pharmacology to demonstrate that chlorogenic acid significantly

ameliorates liver pathological damage and hepatocyte apoptosis through the TLR4/NF-κB pathway, exhibiting notable anti-inflammatory properties.[27] Their study revealed the biological activity and mechanism of chlorogenic acid in treating septic acute liver injury. The concept of molecular docking is a computer-aided drug design technology that relies on computer-simulated structural methods.[28] By predicting the binding between compounds and targets, it verifies the binding modes and binding energies between chemical components and key targets, thereby enhancing the accuracy of network pharmacological predictions.[29] In this study, network pharmacology and molecular docking methods were used to analyze the relevant targets and pathways of *Dendrobium officinale* in the treatment of liver cancer. Finally, the network pharmacological results were re-validated by an in vitro cellular experimental model, which lays the foundation for the subsequent clinical application of *Dendrobium officinale* in the treatment of hepatocellular carcinoma. The research protocol is illustrated in Figure 1.

Material and Methods

Experimental Cells and Cell Cultures

HepG2 was purchased from Wuhan Purusai. First, the growth status and density of cells in the culture dish were observed, and after confirming that the cells were in good condition, the culture medium and trypsin were preheated in a 37°C water bath. Subsequently, the preheated medium, trypsin and PBS buffer were surface sterilized with 75% alcohol and transferred to an ultra-clean bench for backup. Cell culture dishes were removed from the incubator, the original medium was aspirated, and 2–3 mL of PBS buffer was added to gently rinse the cells twice to remove residual medium

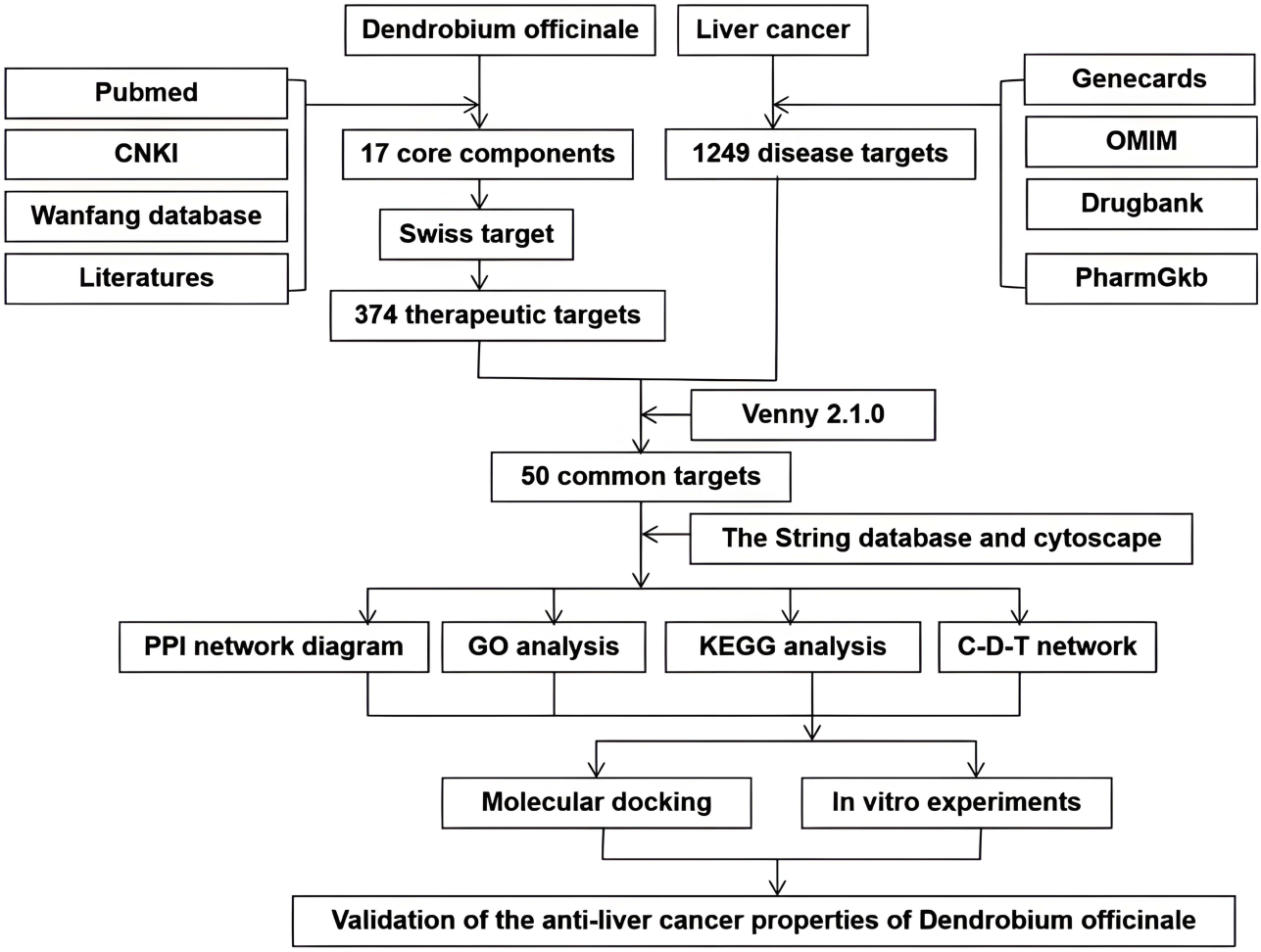

Figure 1 This design diagram illustrates the workflow of integrating network pharmacology and molecular docking, culminating in in vitro experimental validation of the therapeutic efficacy of *Dendrobium officinale* in treating liver cancer.

https://doi.org/10.2147/JHC.S527095

components. After discarding the PBS buffer, add 1 mL of trypsin digestion solution, gently shake the dish to make the trypsin evenly cover the cell layer, and leave it to digest for 2–3 minutes at room temperature. When the whole cell layer was observed to be dislodged by gently shaking the dish, it indicated that the digestion was completed, and 2 mL of fresh medium was added immediately to terminate the digestion reaction. Subsequently, the cell suspension was blown repeatedly using a pipette gun to ensure that the cells were well dispersed. The cell suspension was inoculated into a new petri dish containing 10 mL of fresh medium at a ratio of 1:4, and the dish was gently shaken to distribute the cells evenly. Finally, the cell distribution status was observed under a microscope, and after confirming the uniformity, the culture dish was placed in a 37°C, 5% CO_2 incubator for further cultivation.

Experimental Reagents and Instruments

The aqueous extract of *Dendrobium officinale* was provided by Hunan Zhishengyuan Science and Technology Company. CCK-8 (Elabsciencec, model: E-CK-A362); incubator and pipette gun were purchased from Thermo; AKT1 (model: 20584-1-AP), EGFR (model: 18986-1-AP), CCND1 (model: 26939-1-AP) antibodies were purchased from proteintech; PI3K (proteintech, model: 10176-2-AP); PI3K (proteintech, model: 10176-2-AP) antibodies were purchased from proteintech. 26939-1-AP) antibodies were purchased from proteintech; PI3K (proteintech, model: 10176-2-AP); α-MEM medium (containing ribonucleoside, deoxyribonucleoside, phenol red, and L-glutamine components, model: C12571500BT) was purchased from Gibco; Western and IP cell lysates (Biosharp, model: BL509A); PBS phosphate buffer (Gibco, model: C10010500BT); bench-top high-speed freezing centrifuge (Xiangyi, model: H1650R); centrifuge (Changsha Xiangzhi Centrifuge Instrument Co., Ltd., model: TDZ5-WS); protein blotting (Changsha Xiangzhi Centrifuge Instrument Co., Ltd., model: TDZ5-WS); protein blotting imaging system (cytiva, model: 800); cryogenic refrigerator at minus 80 degrees (Thermo, model: 908GP); electrophoresis instrument (BIO-RAD, model: 165–8033); multifunctional enzyme labeling instrument was purchased from Thermo Company.

Preparation of the Aqueous Extract of Dendrobium officinale

The fresh stem samples of *Dendrobium officinale* used in this study were collected from a local planting cooperative in Xinning County, Shaoyang City, Hunan Province, China. The material was systematically identified as authentic *Dendrobium officinale* by Professor Lu Yibo's team from the Institute of Botany, Chinese Academy of Sciences. The sample pretreatment process was as follows: First, the collected stem segments were dried in an oven at 40°C for 24 hours. Subsequently, they were ground using a mill and passed through a 40-mesh sieve before being stored in a −20°C freezer for later use. Precisely 50 g of the dried sample was accurately weighed and placed in a 1 L round-bottomed flask. Ten volumes of distilled water were added, and the mixture was soaked at room temperature for 12 hours. Then, heat reflux extraction was employed, and the extraction was carried out twice: In the first extraction, the soaked material was boiled for 1 hour and filtered hot through gauze. The filter residue was re-extracted with 10 volumes of distilled water for another 1 hour of reflux. The two extracts were combined and concentrated to 60 mL using a RE-5298 rotary evaporator produced by Shanghai Yitian Scientific Instrument Co., Ltd. Finally, the concentrated solution was frozen overnight in a −80°C ultra-low temperature freezer and then freeze-dried for 12 hours to obtain the final product.

Determination of the Chemical Component Contents in Dendrobium officinale

Determination of Total Flavonoid Content

First, prepare the rutin standard solution and plot the standard curve. Accurately weigh 20 mg of rutin standard substance into a 100 mL volumetric flask, dissolve with an appropriate amount of 70% ethanol, and dilute to 100 mL to obtain a 200 mg/L rutin standard solution. Then, accurately measure different volumes of the standard solution into 15 mL centrifuge tubes, add 3 mL of 70% ethanol and make up to 5 mL. Then, add 0.3 mL of sodium nitrite solution, mix thoroughly, and let stand for 8 minutes; add 0.3 mL of aluminum chloride solution, shake well, and let stand for 10 minutes; add 4.0 mL of sodium hydroxide solution, then make up to the mark with ethanol solution, shake well, and let stand for 10 minutes. Finally, plot a standard curve with rutin concentration as the x-axis and absorbance as the y-axis. Then, the extraction of total flavonoids from *Dendrobium officinale* was conducted. We weighed 0.5 g of *Dendrobium*

officinale powder, added 10 mL of 80% ethanol, and extracted it in a 60°C water bath for 3 hours. We filtered the filtrate, diluted it to 25 mL with ethanol solution, and let it stand for testing.

Determination of Polyphenol Content

First, prepare a gallic acid standard curve. Weigh 20 mg of gallic acid into a brown volumetric flask, dissolve with distilled water, and dilute to 100 mL to prepare a 200 mg/L standard solution. Transfer different volumes of the standard solution into 15 mL centrifuge tubes wrapped in aluminum foil. Add 60% ethanol solution to make up to 10 mL to obtain the working solution. Take 1.0 mL of the working solution, add 2.5 mL of phenol-chlorophenol-chlorothionol reagent, 2.5 mL of 15% Na_2CO_3 solution, and dilute with water to 10 mL. Mix well and incubate at 40°C for 60 minutes, then let cool for 20 minutes. Measure the absorbance at 778 nm using an enzyme-linked immunosorbent assay (ELISA) reader. Plot the working solution concentration on the x-axis and absorbance on the y-axis. Next, determine the total phenolic content. Take 100 mg of the prepared powder, extract with 10 mL of 80% ethanol solution for 24 hours, filter, and centrifuge at 3500 rpm for 20 minutes. Take the supernatant and set it aside. Add 80% ethanol solution to make up to 25 mL, and determine the total phenolic content using the above method and calculate it based on the standard curve. Finally, determine the total polyphenol content of *Dendrobium officinale*. Weigh 0.5 g of *Dendrobium officinale*, add 30 mL of 60% ethanol, and sonicate for 10 minutes. Dilute to 50 mL with 60% ethanol, shake well, filter, and determine the content using the method described above.

Screening of Candidate Compounds and Targets of Dendrobium officinale

Setting "Dendrobium officinale" "ingredient" as the search keywords. By searching for target literature in the PubMed databases (https://pubmed.ncbi.nlm.nih.gov/), CNKI (https://www.cnki.net/index/), Wanfang (https://www.wanfangdata.com.cn/) and other databases, obtain information on the chemical components of *Dendrobium officinale*. After categorizing and organizing the data, remove duplicates and conduct an initial screening. In the Traditional Chinese Medicine Systems Pharmacology Database and Analysis Platform (https://old.tcmsp-e.com/tcmsp.php), further filter the data based on the criteria of Oral Bioavailability (OB)≥ 30% and Drug-likeness (DL)≥ 0.18.[30] The effective components obtained after filtering are then imported into the PubChem (https://pubchem.ncbi.nlm.nih.gov/) website to retrieve their SMILES codes. Using the Swiss ADME database (http://www.swissadme.ch/), compounds are screened based on having at least 2 YESes in the high Gastrointestinal Absorption and drug-likeness principles. Ultimately, the core compounds of *Dendrobium officinale* are collected. Subsequently, the SwissTarget Prediction (http://swisstargetprediction.ch/) database is used to predict the targets of these active components, with the species set to "Homo sapiens" and the condition set to "Probability > 0.1". The target information is then converted into gene names using the UniProt database (https://www.uniprot.org/).

Screening of Disease Targets and Intersection Genes

Using the GeneCards (https://www.genecards.org/) database, DRUGBANK (https://go.drugbank.com/) database, OMIM (https://www.omim.org/) database, and PharmGkb (https://www.pharmgkb.org/) database, the keyword "Liver cancer" is entered to retrieve potential disease targets for liver cancer. By merging the data from these four disease databases and removing duplicate values, a list of potential targets for liver cancer is obtained. The drug component targets and disease targets obtained from the above steps are uploaded to the Venny 2.1.0 (https://bioinfogp.cnb.csic.es/tools/venny/) platform to identify the intersection genes.

Construction of PPI Network and Selection of Core Targets

Using the STRING (https://cn.string-db.org/) database, the intersection targets are imported, and "homo sapiens" is selected to perform PPI analysis. The file is saved for further analysis, and the results are visualized using Cytoscape 3.10.1 software. The Centiscape 2.2 plugin within Cytoscape software is utilized to calculate the degree, BC, and CC of the targets. The top 10 genes ranked by degree value are selected as the core targets.

GO Functional and KEGG Pathway Enrichment Analysis

The intersection genes are imported into the David (https://david.ncifcrf.gov/) database for GO functional annotation and KEGG pathway enrichment analysis. With a significance threshold of $P<0.05$, the top 10 results in BP, MF, and CC categories, as well as the top 20 results from the KEGG pathway enrichment analysis, are selected. The GO enrichment bar chart and KEGG enrichment bubble chart are then plotted using the Weishengxin (http://www.bioinformatics.com.cn/) platform.

Construct an Ingredient-Target-Disease Pathway Network Diagram

The compounds, intersecting targets and the top 20 key pathways screened by KEGG enrichment analysis of *Dendrobium officinale* were integrated and imported into Cytoscape software to construct a multidimensional network topology map of "drug-component-target-pathway". Through visual analysis, the complex interaction between *Dendrobium* components and intersecting targets and major signaling pathways was revealed. In the network diagram, the size of a node is positively correlated with its importance in the network, and the larger the node is, the more significant its core role in the network is.

Molecular Docking Verification

Firstly, the compound structure files (SDF format) of *Dendrobium officinale* were retrieved and downloaded from the PubChem database, and subsequently the SDF files were converted to PDB format using Open Babel 2.3.2 software. Meanwhile, the protein crystal structure files of the core targets were obtained from the RCSB PDB database. The receptor proteins were pre-processed using PYMOL 2.3.4 software, including the removal of water molecules, ligands and other components. Next, the receptor proteins were subjected to hydrogenation and charge balance optimization by AutoDockTools software, and the receptor proteins and ligand small molecules were converted to PDBQT format, respectively. Molecular docking calculations were performed using AutoDock Vina 1.1.2 software to verify the binding ability of the active ingredients to the core target, and the interaction details in the docking results were analyzed using PLIP (Protein–Ligand Interaction Profiler) tool. Finally, the molecular docking results of the key ingredients with the core targets were visualized based on the PyMol platform, which intuitively presented the binding mode and interaction characteristics.

Using the CCK-8 to Assess the Effect of Aqueous Extract of Dendrobium officinale on the Viability of HepG2 Cells

HepG2 cell suspensions were inoculated in 96-well plates with a cell density of 2×10^4 cells per well and placed in a 37°C incubator for 24 h to allow the cells to fully adhere to the wall. Subsequently, different concentration gradients of *Dendrobium* aqueous extracts were added to each well separately and continued to be incubated at 37°C in the incubator for 24 hours. At the end of incubation, 10 μL of CCK-8 solution was added to each well, taking care to avoid air bubbles, and then the 96-well plate was placed back into the 37°C incubator for 2 hours. The experiments were set up with a blank group (containing medium only, no cells and drugs) and a control group (containing cells, no drugs) as reference. The absorbance value (OD value) of each well was measured at 450 nm using an enzyme labeling apparatus, and each group of experiments was repeated at least three times. Cell survival rate(%) = $(OD_{sample}\text{-}OD_{blank})/(OD_{control}\text{-}OD_{blank}) \times 100\%$.

Western Blotting Analysis Is Used to Detect the Expression of p-PI3K/PI3K, AKT1, EGFR, and CCND1 in Related Pathways

Pretreatment of Samples

Cells were plated in a 6-well plate and cultured for 24 hours, followed by an additional 2.5 hours of culture in serum-free medium. After that, different concentrations of *Dendrobium officinale* aqueous extract were added and the cells were incubated for another 24 hours. Upon completion of the treatment, the culture dishes were placed on ice, and the medium was aspirated using a pipette. The cells were then washed 2–3 times with ice-cold PBS buffer. After aspirating the PBS buffer completely, 150–200 μL of 2% SDS solution was added evenly to each well, and the cells were incubated on ice for 10–20 minutes to ensure complete lysis. After lysis, the lysate was transferred into a 1.5 mL centrifuge tube for subsequent Western blot analysis.

Western Blotting Analysis

A certain volume of 5× protein uploading buffer was added proportionally to the EP tube containing the lysate, and after thorough mixing, the sample was denatured by heating in a 100°C metal bath for 10 minutes. Subsequently, once the sample cooled slightly, the protein sample was loaded into a 10% SDS-PAGE gel. After electrophoresis was completed, the gel was cut, and then transferred to a membrane at a constant current of 250 mA. Once the transfer was complete, the PVDF membrane was placed in TBST sealing solution containing 3–5% skimmed milk for 1 hour. After sealing, the membrane was washed three times with TBST on a shaker for 5 minutes each time. After the membrane was washed, the primary antibody was diluted with antibody diluent, incubated overnight at 4°C, and washed three times with TBST on a shaker for 5 minutes each time. The corresponding secondary antibody was added, the secondary antibody was diluted with the sealing solution, incubated at room temperature for 2 hours, and then the membrane was washed three times with TBST on a shaker for 5 minutes each time. A certain amount of freshly prepared ECL chemiluminescent substrate was added to the PVDF membrane. The membrane was then exposed and imaged using an Image Quant LAS 8000 gel imaging system. Finally, protein bands were quantitatively analyzed using ImageJ software.

Statistics and Analysis

The experimental data were expressed as mean ± standard deviation. Statistical analysis was performed with GraphPad Prism software, one-way ANOVA was used for comparisons between multiple groups, and *t*-test was used for comparisons between two groups of data, with $P<0.05$ indicating that the difference was statistically significant.

Results

Predicted results of Candidate Compounds and Targets of Dendrobium officinale

Using multiple databases and literature search, a total of 512 chemical components related to *Dendrobium officinale* were collected, and 17 key ingredients were obtained through layer-by-layer screening. The specific ingredients are shown in Table 1. Using the Swiss Target Prediction database for ingredient target prediction, we merged the drug targets and removed duplicates, ultimately obtaining 374 drug targets.

Table 1 17 Kinds of Active Ingredients Have Been Identified from the Extract of *Dendrobium Officinale*

Number	Molecule Name	Chemical Formula	MW (g/mol)	OB (%)	DL
DO1	N-p-Coumaroyltyramine	$C_{17}H_{17}NO_3$	283.35	112.90	0.20
DO2	Medioresinol	$C_{21}H_{24}O_7$	388.45	87.19	0.62
DO3	Moupinamide	$C_{18}H_{19}NO_4$	313.38	86.71	0.26
DO4	Eriodictyol	$C_{10}H_{11}NO_3$	288.27	71.79	0.24
DO5	Butin	$C_{15}H_{12}O_5$	272.27	69.94	0.21
DO6	Sophoranol	$C_{15}H_{24}N_2O_2$	264.41	67.32	0.28
DO7	Isorhamnetin	$C_{16}H_{12}O_7$	316.28	49.60	0.31
DO8	Triptophenolide	$C_{20}H_{24}O_3$	312.44	48.50	0.44
DO9	5-methyl-7-methoxyisoflavone	$C_{17}H_{14}O_3$	266.31	42.56	0.20
DO10	Skimmin	$C_{15}H_{16}O_8$	324.31	38.35	0.32
DO11	Sanguinarine	$C_{20}H_{14}NO_4^+$	332.35	37.81	0.86
DO12	Alpha-Glyceryl linoleate	$C_{21}H_{38}O_4$	354.59	37.18	0.30
DO13	Luteolin	$C_{15}H_{10}O_6$	286.25	36.16	0.25
DO14	Chryseriol	$C_{16}H_{12}O_6$	300.28	35.85	0.27
DO15	Acacetin	$C_{16}H_{12}O_5$	284.28	34.97	0.24
DO16	Hispidulin	$C_{16}H_{12}O_6$	300.28	30.97	0.27
DO17	Isolupalbigenin	$C_{25}H_{26}O_5$	406.47	30.68	0.23

Notes: DO *Dendrobium officinale*, MW molecular weight, OB oral bioavailability, DL drug-likeness.

Acquisition of Intersection Targets and PPI Network Analysis

We retrieved a total of 1,370 disease targets from four databases: GeneCards, DRUGBANK, OMIM, and PharmGkb Specifically, we obtained 573 disease targets from GeneCards, 6 from DRUGBANK, 508 from OMIM, and 283 from PharmGkb. Then, using Excel tools, we integrated and removed duplicates to obtain a final list of 1,249 disease gene targets. By importing the 374 component targets and the 1,249 disease targets into Venny 2.1.0 software, we identified a total of 50 intersection targets, as shown in Figure 2A. With the help of String database, the intersecting genes were imported into it to construct the PPI network diagram. Then, the downloaded file was further imported into Cytoscape 3.10.1 software, and the parameters of the nodes were set to be greater than the median value (Degree>20.612, Closeness>0.013, Betweenness>30.204) using Centiscape2.2 plug-in, and the core targets with the top 10 filtering degree values are as follows AKT1, CCND1, EGFR, HIF1A, SRC, PPARG, PTGS2, MMP9, JAK2, TERT, as shown in Figure 2B and C. The candidate components of *Dendrobium officinale* corresponding to these targets are Butin, Skimmin, N-p-Coumaroyltyramine, Moupinamide, Sophoranol, and Isorhamnetin, as detailed in Table 2.

Results of GO and KEGG Pathway Functional Enrichment Analysis

Using the David database, the intersection targets were input, and the reference value of $P<0.05$ was set for GO function and KEGG pathway enrichment analysis. A total of 397 entries were obtained from the GO function enrichment, including 284 entries for BP, 75 entries for MF and 38 entries for CC. The top 10 enriched results for each category were selected to create bar charts, as shown in Figure 3A (the horizontal coordinates represent the names of the three enriched functional processes, and the vertical coordinates represent the number of entries enriched in each GO function). The top 5 BP entries include positive regulation of phosphatidylinositol 3-kinase signaling, protein autophosphorylation, positive regulation of protein kinase B signaling, positive regulation of kinase activity, and transmembrane receptor protein

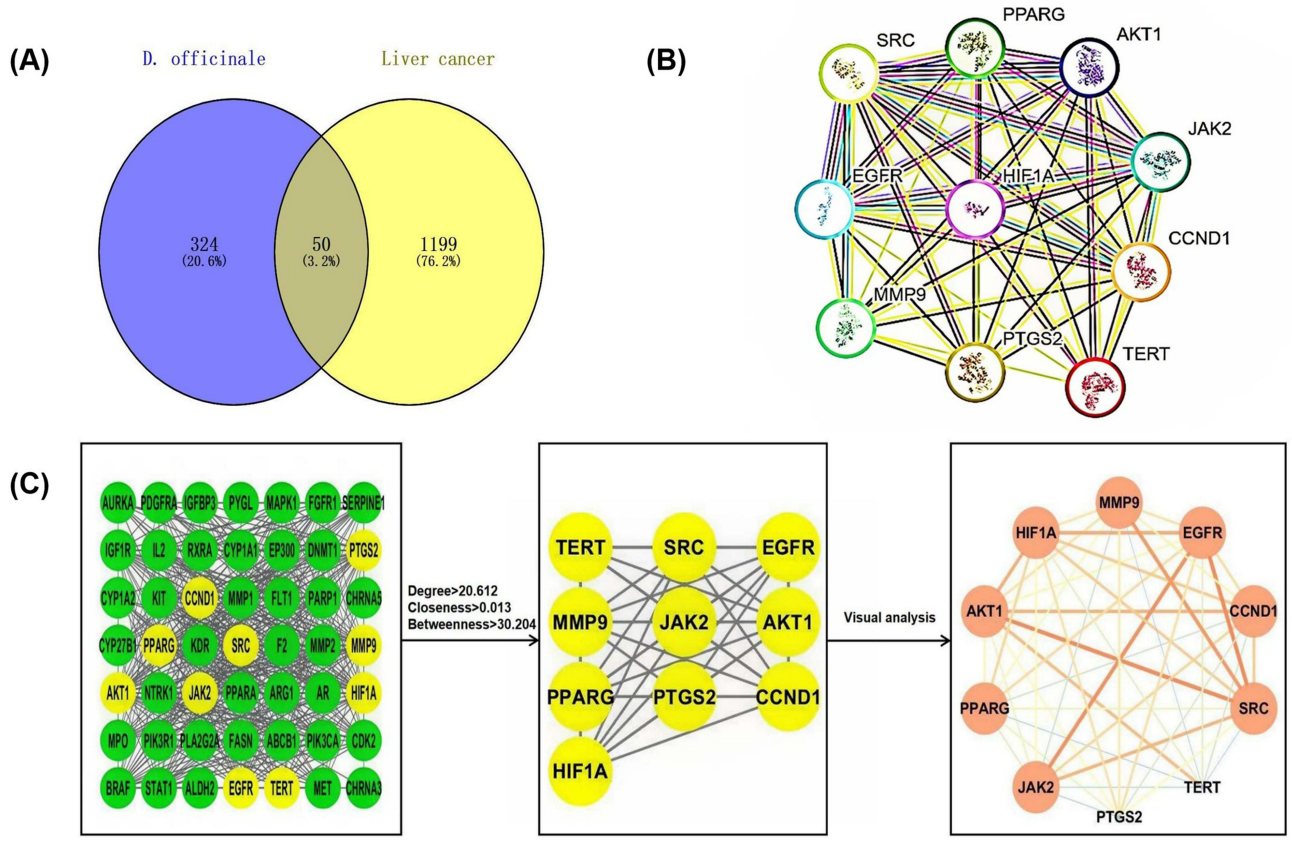

Figure 2 (**A**) A Venn diagram highlighting the overlap between the active components of *Dendrobium officinale* and liver cancer-related targets, (**B**) Protein–Protein Interaction, (**C**) Flowchart for Core Target Screening.

Table 2 TOP10 Target Information

Number	Gene Sympol	Degree	Betweenness	Closeness	Molecule
1	AKT1	41	173.627671	0.018181818	Butin
2	CCND1	38	77.11482828	0.017241379	Skimmin
3	EGFR	38	97.31414285	0.017241379	N-p-Coumaroyltyramine
4	HIF1A	38	95.36346122	0.016949153	Butin
5	SRC	35	69.27388344	0.016129032	Butin
6	PPARG	35	75.82978808	0.016393443	Butin
7	PTGS2	33	68.87938548	0.015625	Moupinamide
8	MMP9	33	40.74553567	0.015625	N-p-Coumaroyltyramine
9	JAK2	31	100.5678194	0.015151515	Sophoranol
10	TERT	24	128.5214893	0.013888889	Isorhamnetin

tyrosine kinase signaling pathway. The top 5 MF entries are protein serine/threonine/tyrosine kinase activity, protein tyrosine kinase activity, transmembrane receptor protein tyrosine kinase activity, enzyme binding, and ATP binding. The top 5 CC entries include receptor complex, caveola, macromolecular complex, nucleus, and nucleoplasm.

The drug-disease intersection targets were subjected to KEGG pathway enrichment analysis, and a total of 129 meaningful pathways were obtained, and the top 20 pathway enrichment information was selected to draw a bubble map, as shown in Figure 3B. The mainly involved enriched pathways included Pathways in cancer, Prostate cancer, EGFR tyrosine kinase inhibitor resistance, Proteoglycans in cancer, and PI3K-AKT signaling pathway.

Results of the Construction of the Network Diagram of "Traditional Chinese Medicine - Component - Target – Disease Pathway"

Using Cytoscape software, the drug ingredients, intersection targets, and the top 20 KEGG enriched pathways were imported together for network topology analysis and visualization processing. The results are shown in Figure 4. The network diagram consists of 89 nodes (including 17 candidate compounds, 50 intersection targets, 20 major pathways, and one each for traditional Chinese medicine and disease name) and 339 edges. In this diagram, orange represents drug ingredients, green represents KEGG pathways, and blue represents the targets. The size of nodes is set according to the Degree value: the larger the node, the darker the color, which means the larger the Degree value.

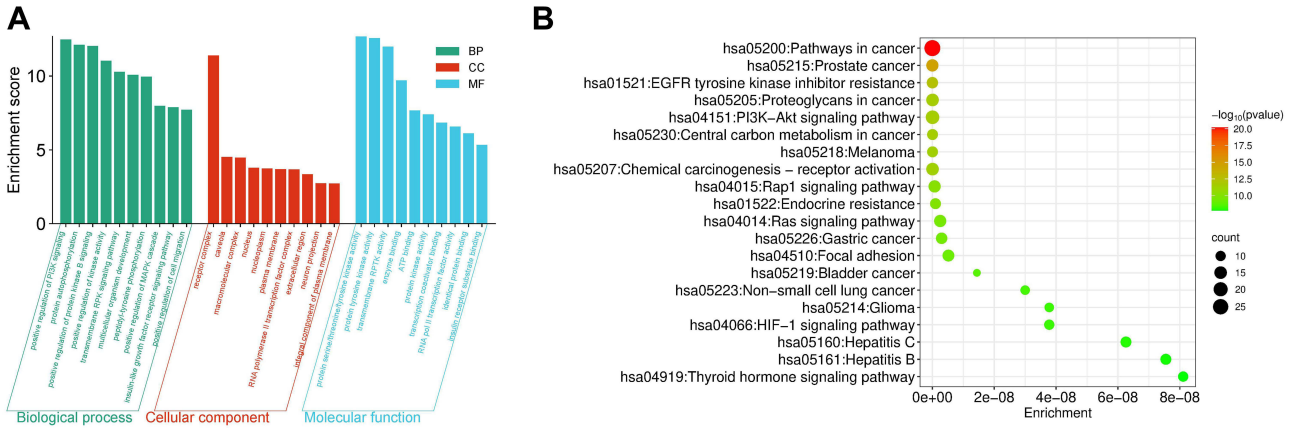

Figure 3 (**A**) The enrichment analysis bar chart of the top 10 Gene Ontology (GO) categories, BP biological process, CC cellular component, MF molecular function, (**B**) The KEGG Enrichment Bubble Chart for the Top 20 Pathways.

https://doi.org/10.2147/JHC.S527095

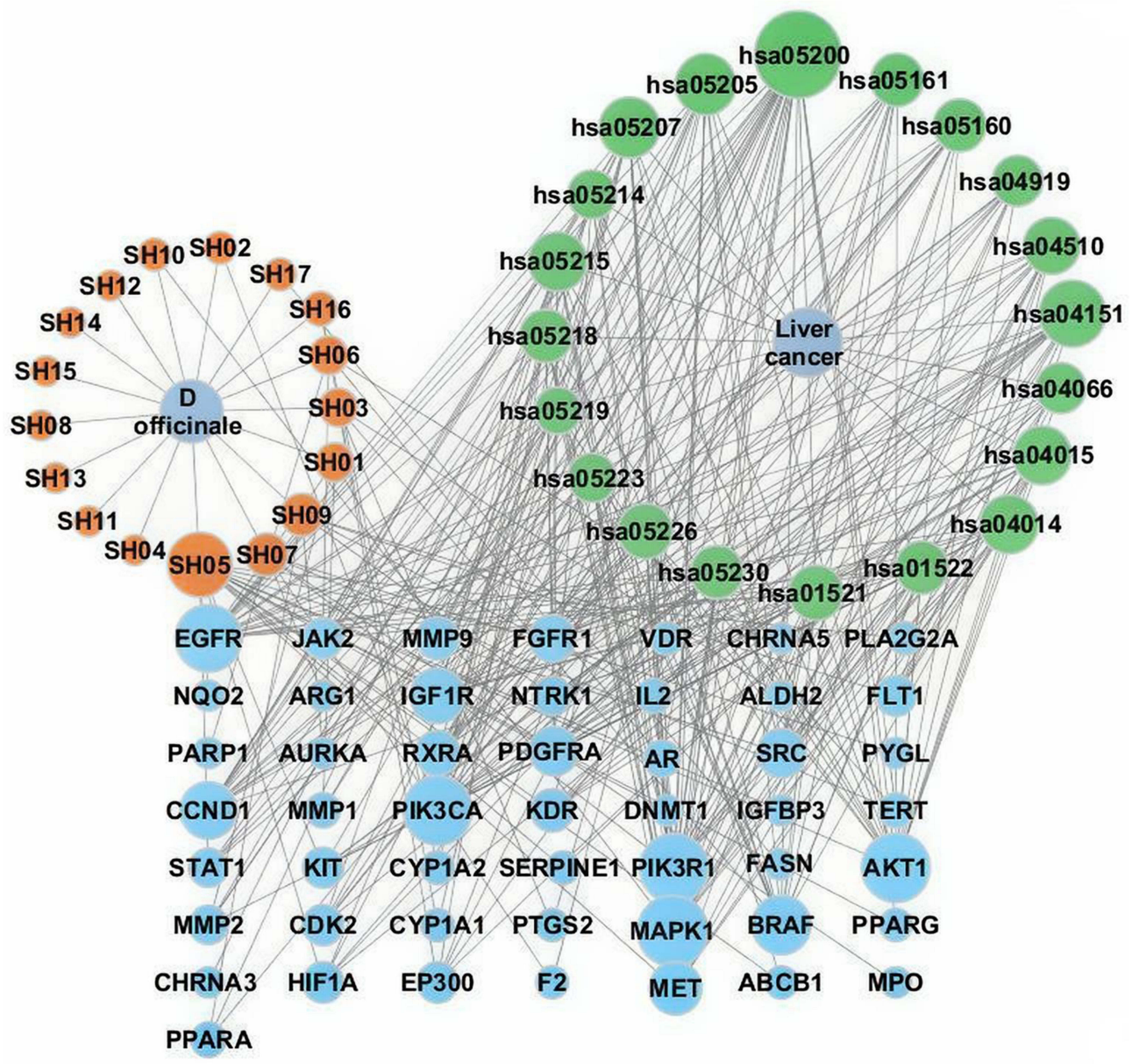

Figure 4 The network diagram of "TCM - Component - Target - Disease Pathway".

Molecular Docking Analysis

The top 3 core targets (AKT1, CCND1, EGFR) were used as the target proteins for molecular docking, and the 3 core components with the highest Degree value (Butin, skimmin, N-p-Coumaroyltyramine) were selected as the small molecules for molecular docking, and the AutoDock Vina 1.1.2 software was applied to carry out molecular docking. The simulation results showed that stable binding was formed between these components and the core target, indicating that they have good binding affinity for each other, and the binding energy results of each group are shown in Table 3. The molecular docking reflects the degree of conformational stability of the small molecules bound to the receptor proteins, and the smaller the binding energy is, the better the docking degree is. A binding energy less than −5.0 kcal/mol implies a good binding affinity of the ligand and the target proteins, while the binding energy less than −7.0 kcal/mol indicates the strong binding activity of ligand and the receptor.[31,32] The top 6 complexes ranked by the absolute value of binding energy were selected for visual analysis using PyMol tools, with the results shown in Figure 5. Among them, the

Table 3 The Molecular Docking Results of Core Components and Core Targets

Protein	Molecule	Binding Energy (kal/mol)
AKT1	Butin	−10.8
AKT1	N-p-Coumaroyltyramine	−8.4
AKT1	Skimmin	−9.1
CCND1	Butin	−5.9
CCND1	N-p-Coumaroyltyramine	−5.6
CCND1	Skimmin	−6.0
EGFR	Butin	−7.7
EGFR	N-p-Coumaroyltyramine	−7.0
EGFR	Skimmin	−7.2

molecules Butin, N-p-Coumaroyltyramine, and skimmin had the best docking activity with the gene AKT1, and the molecular docking heatmap is shown in Figure 6, with darker color indicating better docking activity.

Chemical Composition Analysis of Dendrobium officinale

Total Flavonoid Content Analysis

By analyzing the obtained data, the following standard curve for total flavonoids was obtained, with the corresponding linear equation being: $y = 0.0012x + 0.0012$, $R^2 = 0.9882$, indicating a relatively good data relationship. The units on the X-axis are rutin concentration (mg/mL), and the units on the Y-axis are the corresponding absorbance values. The total flavonoid content in *Dendrobium officinale* was measured to be 5.78 ± 0.24 mg/g. The results are shown in Figure 7.

Total Polyphenol Content Analysis

The collected data were analyzed to obtain the following total polyphenol standard curve. The corresponding linear equation was $y = 0.0102x - 0.0162$, with $R^2 = 0.985$, indicating a relatively good data relationship. The X-axis units represent gallic acid concentration (mg/mL), and the Y-axis represents the corresponding absorbance values. The total polyphenol content in the *Dendrobium officinale* extract was measured to be 11.21 ± 0.76 mg/g. The results are shown in Figure 8.

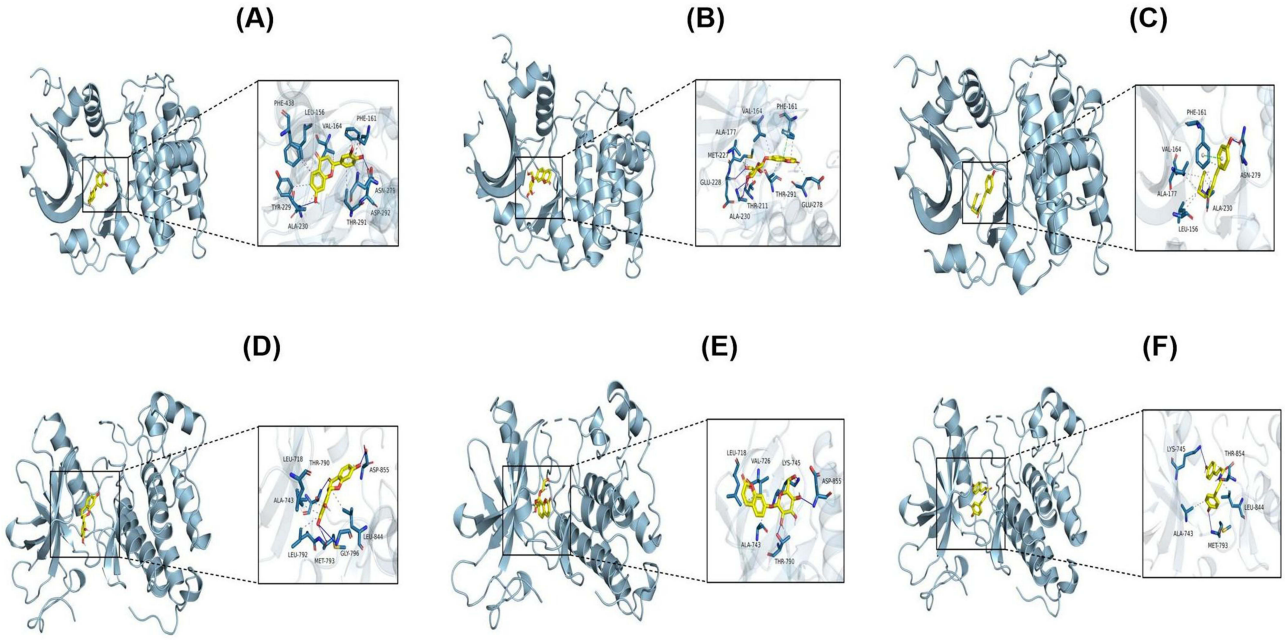

Figure 5 Molecular docking mode diagrams of some core compounds. (**A**) Docking diagram of AKT1 with Butin, (**B**) Docking diagram of AKT1 with Skimmin, (**C**) Docking diagram of AKT1 with N-p-Coumaroyltyramine, (**D**) Docking diagram of EGFR with Butin, (**E**) Docking diagram of EGFR with Skimmin, (**F**) Docking diagram of EGFR with N-p-Coumaroyltyramine.

https://doi.org/10.2147/JHC.S527095

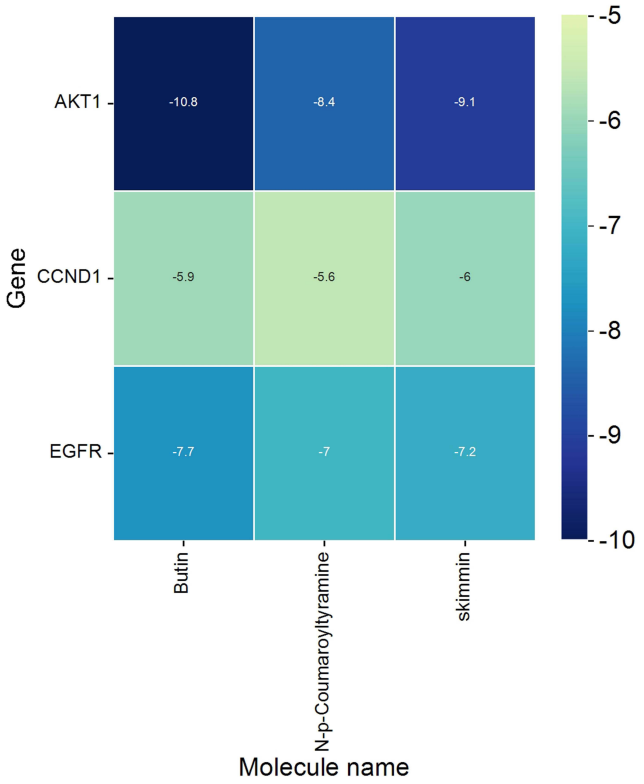

Figure 6 Heatmap of binding energy matrix between active components of *Dendrobium officinale* and liver cancer targets.

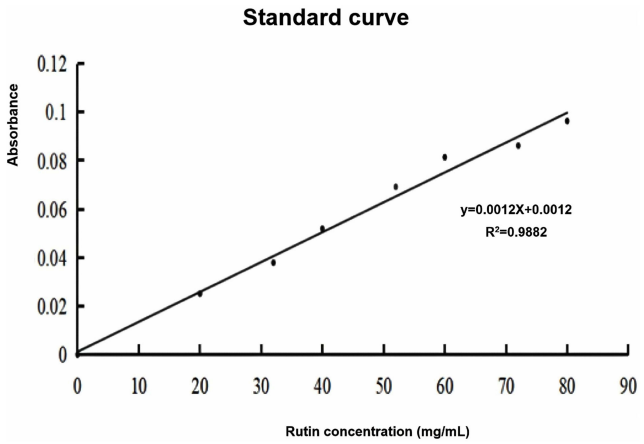

Figure 7 Rutin solution standard curve.

The Effect of Aqueous Extract of Dendrobium officinale on the Proliferation of HepG2 Cells

The results of CCK-8 assay showed that different concentrations (0.5, 1, 2, 4 and 8 mg/mL) of *Dendrobium* aqueous extracts were able to significantly inhibit the proliferative activity of HepG2 cells and induced cell cycle arrest after treating HepG2 cells for 24 h compared with the control group (0 mg/mL), and this inhibitory effect showed a significant dose-dependence. Specifically, when the concentration of Dendrobium aqueous extract reached 2 mg/mL and above, the cellular activity was significantly reduced ($P<0.05$), indicating that Dendrobium aqueous extract had a significant antiproliferative effect on HepG2 cells at higher concentrations. Through the dose-effect curve analysis, the half-maximum inhibitory concentration (IC50) of Dendrobium aqueous extract for inhibiting the proliferation of HepG2

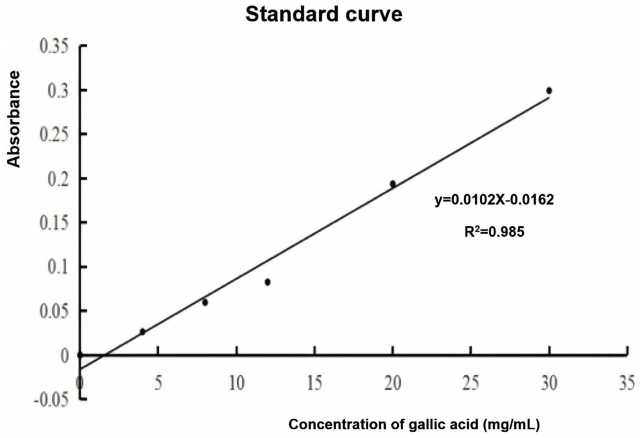

Figure 8 Standard curve for gallic acid solution.

cells was calculated to be 5.755 mg/mL, and this result further confirmed the inhibitory effect of Dendrobium aqueous extract on HepG2 cells. The experimental results are shown in Figure 9.

Effects of Aqueous Extracts of Dendrobium officinale on the Expression of Core Proteins p-PI3K/PI3K, AKT1, CCND1 and EGFR in Related Pathways

To conduct a Western blotting analysis, different concentrations of *Dendrobium officinale* aqueous extract (1, 2, and 4 mg/mL) were selected as the low, medium, and high dose groups, respectively, to verify the expression activity of core proteins AKT1, EGFR, CCND1, and p-PI3K/PI3K in HepG2 cells under the treatment of *Dendrobium officinale* aqueous extract. GAPDH was used as the internal reference protein. The Control group served as the negative control group. Compared with the Control group, the protein expression levels of AKT1, CCND1, and EGFR, as well as the relative expression of p-PI3K/PI3K protein, in HepG2 cells of the low, medium, and high dose groups were all lower than those in the Control group, with statistically significant differences ($p<0.05$). These results suggest that *Dendrobium officinale* aqueous extract inhibits the expression of the PI3K/AKT signaling pathway by downregulating the protein expression levels of p-PI3K/PI3K and AKT1, which is illustrated in Figure 10.

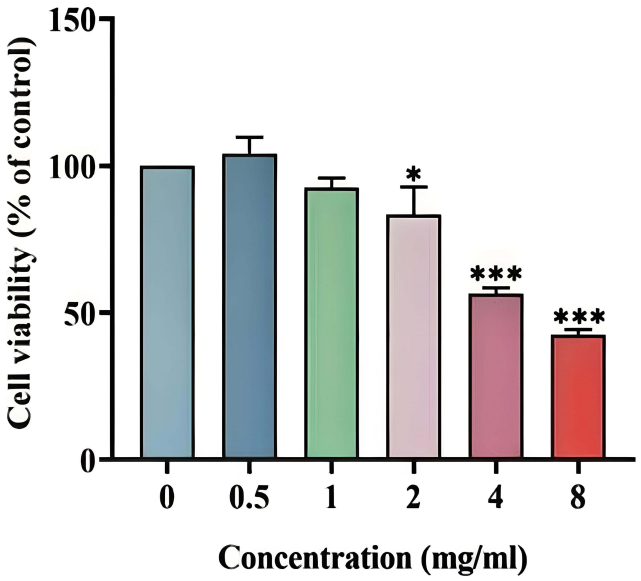

Figure 9 Inhibitory effect of aqueous extract of *Dendrobium officinale* on the proliferation of HepG2 cells. Compared with the control group, *$p<0.05$, ***$p<0.001$.

https://doi.org/10.2147/JHC.S527095

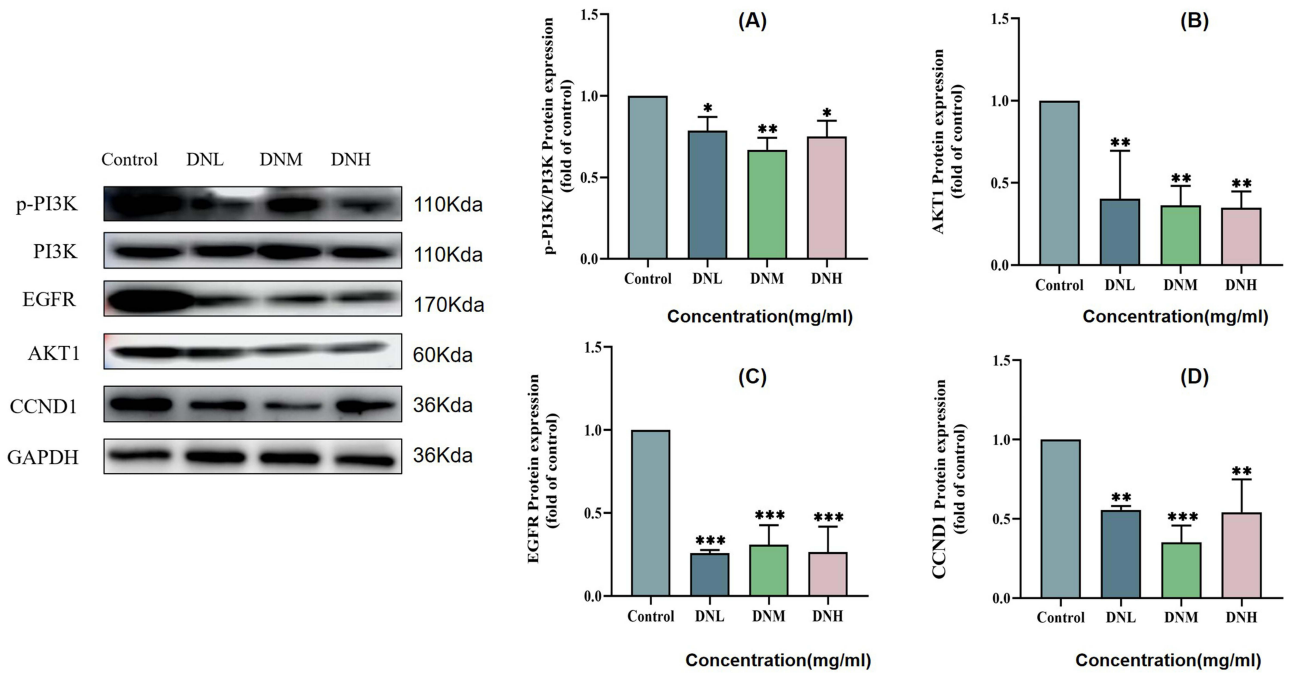

Figure 10 The aqueous extract of *Dendrobium officinale* exerts an anti-liver cancer effect by down regulating the protein expression levels of p-PI3K/PI3K, AKT1, EGFR, and CCND1. The protein expression levels of (**A**) p-PI3K/PI3K, (**B**) AKT1, (**C**) EGFR, and (**D**) CCND1 were determined by Western blotting. DNL, DNM, DNH vs Control, **p*<0.05, ***p*<0.01, and ****p*<0.001.

Discussion

Primary liver cancer, originating from malignant transformations within liver tissue, was the third leading cause of death globally in 2020,[33] with an increasing incidence annually. The latest projected trends indicate a continuous rise in new liver cancer cases, expected to surge from approximately 905,347 cases to an estimated 1,392,474 cases by 2040.[34] The treatment of patients with early-stage tumors is still based on surgery, but the 5-year recurrence rate after surgery reaches 40%–70%,[35] and postoperative high-risk recurrence factors include tumors with a diameter of 5 centimeters or larger, vascular infiltration, multiple tumors, satellite nodules, and poorly differentiated tumors.[36] In addition, postoperative complications and poor prognosis are still the most urgent problems surgeons need to address at present. For patients with advanced tumors, systemic interventions are often relied upon, which include transarterial chemoembolization, cytotoxic chemotherapy, targeted therapy, and immunotherapy.[37,38] However, most patients fail to achieve significant clinical remission. Although drugs like sorafenib and lenvatinib offer some degree of efficacy in treating liver cancer, their benefits are limited. In recent years, with the rising international recognition of traditional Chinese medicine and herbal remedies, numerous studies have demonstrated the anti-hepatocellular carcinoma properties of *Dendrobium officinale*, although its underlying mechanisms of action remain to be elucidated in detail.

Therefore, in our study, a total of 17 candidate components of Dendrobium were screened out using network pharmacology, including Butin, N-p-Coumaroyltyramine, skimmin, etc. The above core components were used as ligands for molecular docking experiments with the core protein receptors in the PPI network diagram, and then the targets and core pathway of Dendrobium was verified with the help of in vitro cellular experiments. The core pathways acting on liver cancer were verified, and the mechanism of action of *Dendrobium officinale* in the treatment of HepG2 cells was concluded. Our research also indicates that *Dendrobium officinale* holds promising potential as a candidate for further development into anticancer drugs with bright prospect in this field.

Through the analysis and screening of the PPI network topology, 10 core targets for the treatment of liver cancer with *Dendrobium officinale* were identified, namely AKT1, CCND1, EGFR, HIF1A, SRC, PPARG, PTGS2, MMP9, JAK2, and TERT. The components of *Dendrobium officinale* can stably dock with these targets, among which the top three targets (AKT1, EGFR, and CCND1) exhibit the highest docking activity. AKT1 is a protein kinase involved in various biological processes in the organism and plays a crucial role in regulating the proliferation, differentiation, invasion and apoptosis of tumor cell,[39] which belongs to the AKT kinase family.[40] Early inhibition of AKT1 activity can reduce tumor cell proliferation and promote apoptosis of liver cancer cells, thereby achieving the purpose of treating liver cancer.[41,42] EGFR is an important regulator that promotes

angiogenesis,[43] which is greatly associated with the angiogenesis of liver cancer.[44] Therefore, the expression of EGFR target proteins promotes cancer cell apoptosis, inhibits tumor proliferation and prevents neovascularization. Many studies have shown that CCND1 is a tumor-associated gene, and CCND1, a cell cycle protein that promotes the cell cycle transition from G1 to S phase,[45–47] was accidentally discovered in 1991.[48] Overexpression of CCND1 can induce continuous proliferation and migration of tumor cells, causing cell cycle arrest in the S phase.[45] Therefore, inhibiting the overexpression of CCND1 may be a promising therapeutic target to exert anti-liver cancer effects. A study has shown that CCND1 is highly expressed in liver cancer tissues, and Ultrasound-Targeted Microbubble Destruction (UTMD)-mediated si-CyclinD1 induces HepG2 cell apoptosis by inhibiting the expression of the PI3K/AKT signaling pathway.[49]

GO functional analysis was performed on the core genes obtained from the PPI network diagram. The BP implicated in the anti-liver cancer effects of *Dendrobium officinale* primarily include positive regulation of PI3K signaling, protein autophosphorylation, and positive regulation of AKT signaling. KEGG enrichment analysis revealed that the top five signaling pathways are closely associated with the anti-liver cancer effects of *Dendrobium officinale*, encompassing Pathways in cancer, prostate cancer, EGFR tyrosine kinase inhibitor resistance, the PI3K-Akt signaling pathway, and proteoglycans in cancer. Among these, the PI3K-Akt signaling pathway, which was also corroborated in the GO functional analysis, exhibits a significant correlation with the positive regulation of PI3K and AKT signaling. Furthermore, the top three target proteins identified in this study, namely AKT, CCND1, and EGFR, are strongly associated with the PI3K-Akt signaling pathway. The PI3K-Akt signaling pathway is a pivotal cellular signaling pathway implicated in various cancer types. In cancer, the overactivation of the PI3K-Akt signaling pathway can promote tumor cell growth and proliferation, inhibit apoptosis, and accelerate malignant progression. Within the PI3K-Akt signaling pathway, growth factors such as insulin-like growth factors and EGFR act as upstream signaling molecules that first bind to specific receptors on the cell membrane, inducing conformational changes in the receptors and initiating intracellular signal transduction, ultimately leading to the activation of PI3K. Dong et al demonstrated that the PI3K-Akt signaling pathway is actively expressed in HCC patients and negatively regulates Fork head box protein O1 (FoxO1). By inhibiting the transcription process of FoxO1, it induces epithelial–mesenchymal transition (EMT) and dysregulation of transforming growth factor-β (TGF-β) expression, ultimately resulting in cancer cell invasion and metastasis to other tissues.[50] Luo et al showed that downregulating the expression of the α-Enolase (ENO1) gene and the PI3K-Akt signaling pathway can impede the growth and spread of HCC cells.[51]

To elucidate the anti-liver cancer mechanism of *Dendrobium officinale*, this study conducted in vitro experiments for verification. In this study, the HepG2 cell line was selected as the experimental model, and the CCK-8 method was used to determine the proliferation of HepG2 cells. Western blotting experiments were performed to assess the expression of proteins related to the pathways. The cellular experimental results demonstrated that *Dendrobium officinale* significantly inhibits the proliferation of HepG2 cells in a dose-dependent manner. Combining the predictions from network pharmacology and molecular docking, the expression activity of core proteins EGFR, AKT1, CCND1, and p-PI3K/PI3K in the relevant pathways was predicted. It was found that the aqueous extract of *Dendrobium officinale* significantly inhibits the activity of proteins such as AKT1 and downregulates the expression levels of PI3K and p-PI3K proteins, thereby inhibiting the expression of the PI3K/AKT signaling pathway and exerting an anti-liver cancer effect.

In summary, this study preliminarily explored the candidate components and core targets of *Dendrobium officinale* in the treatment of liver cancer through network pharmacology and molecular docking. The mechanism of action of *Dendrobium officinale* in liver cancer treatment was identified. Based on this, cellular experiments were conducted to verify the expression of core targets and pathways. Ultimately, it is shown that *Dendrobium officinale* down-regulated p-PI3K/PI3K and AKT1 protein expression levels through core components such as Butin, N-p-Coumaroyltyramine, and skimmin, which negatively regulated the PI3K/AKT signaling pathway to exert a therapeutic effect on liver cancer.

Conclusion

In summary, this study systematically investigated the potential mechanism of *Dendrobium officinale* in treating liver cancer through network pharmacology, molecular docking, and in vitro experiments. Through network pharmacology analysis, we identified key bioactive components in *Dendrobium officinale* (including butin, N-p-coumaroyltyramine, and skimmin) and predicted their potential therapeutic targets and disease-associated targets. Second, molecular docking results demonstrated that these key components could stably bind to core target proteins (AKT1, EGFR, and CCND1) with favorable binding energies,

suggesting their direct regulatory effects on related signaling pathways. These findings further validated the network pharmacology predictions and provided molecular-level evidence for *Dendrobium officinale*'s antitumor mechanism. Finally, CCK-8 assays revealed that Dendrobium aqueous extract significantly inhibited HepG2 cell proliferation in a dose-dependent manner. Following 24-hour exposure, HepG2 cell viability was significantly inhibited by Dendrobium aqueous extract at ≥2 mg/mL concentrations ($P< 0.05$). Western blotting analysis demonstrated that the *Dendrobium officinale* aqueous extract significantly suppressed the protein expression of p-PI3K, PI3K, AKT, EGFR, and CCND1 in HepG2 cells. Specifically: EGFR exhibited statistically extremely significant downregulation across low-, medium-, and high-dose groups ($P< 0.001$). CCND1 showed extremely significant reduction in the medium-dose group ($P< 0.001$). These results indicate that *Dendrobium officinale* aqueous extract exerts anti-liver cancer effects by modulating p-PI3K/PI3K, AKT1, CCND1, and EGFR protein expression, thereby inhibiting PI3K-Akt signaling pathway activation. Thus, this study elucidates *Dendrobium officinale*'s multitarget, multicomponent, and multipathway antitumor mechanism, providing crucial experimental evidence for its therapeutic application in liver cancer treatment.

However, this study also has certain limitations. Firstly, the study was only validated in vitro in cells and did not involve in vivo experiments. Future research plans will continue to refine in vivo experiments and clinical trials. Additionally, while network pharmacology predicted multiple signaling pathways, this experiment only validated the PI3K-Akt signaling pathway, neglecting other signaling pathways that may also exhibit anti-liver cancer effects. This requires further investigation and validation. Finally, due to experimental constraints, no cytotoxicity testing was conducted on normal liver cells. In future research plans, we will conduct in-depth studies to further comprehensively assess its safety and mechanism of action.

Abbreviations

PPI, Protein–Protein Interaction; GO, Gene Ontology; KEGG, Kyoto Encyclopedia of Genes and Genomes; CCK-8, Cell Counting Kit-8; HepG2, Human liver cancer cell line; AKT1, Serine/Threonine-protein Kinase1; CCND1, Cyclin-D1; EGFR, Epidermal Growth Factor Receptor; HIF1A, Hypoxia-Inducible Factor 1-Alpha; SRC, Proto-oncogene tyrosine-protein kinase Src; TLR2, Toll-Like Receptor 2; TAMs, Tumor-Associated Macrophages; OB, Oral Bioavailability; DL, Drug-likeness; GI, Gastrointestinal Absorption; SDF, Standard Delay Format; PDB, Protein Data Bank; PBS, Phosphate Buffered Saline; OD, Optical Density; SDS, Sodium Dodecyl Sulfate.

Data Sharing Statement

The datasets used and/or analyzed during the current study are available from the corresponding author Xuan Lin on reasonable request.

Ethics Approval and Consent to Participate

This study is exempt from approval based on national legislation guidelines, such as item 1 and 2 of Article 32 of the Measures for Ethical Review of Life Science and Medical Research Involving Human Subjects dated February 18, 2023, China for the use of publicly available data.

Consent for Publication

The manuscript is approved by all authors for publication.

Acknowledgments

We thank all authors for their contributions.

Author Contributions

All authors made a significant contribution to the work reported, whether that is in the conception, study design, execution, acquisition of data, analysis and interpretation, or in all these areas; took part in drafting, revising or critically reviewing the article; gave final approval of the version to be published; have agreed on the journal to which the article has been submitted; and agree to be accountable for all aspects of the work.

Funding

This work has been supported by the Natural Science Foundation of Hunan Province (grant number: 2023JJ30295).

Disclosure

The authors declare no conflicts of interest in this work.

References

1. Zhou M, Wang H, Zeng X. et al. Mortality, Morbidity, and Risk Factors in China and Its Provinces, 1990-2017: a Systematic Analysis for the Global Burden of Disease Study 2017. *Lancet*. 2019;394(10204):1145–1158. doi:10.1016/S0140-6736(19)30427-1
2. Bray F, Ferlay J, Soerjomataram I, Siegel RL, Torre LA, Jemal A. Global Cancer Statistics 2018: GLOBOCAN Estimates of Incidence and Mortality Worldwide for 36 Cancers in 185 Countries. *CA Cancer J Clin*. 2018;68(6):394–424. doi:10.3322/caac.21492
3. Siegel RL, Miller KD, Wagle NS, Jemal A. Cancer statistics, 2023. *CA Cancer J Clin*. 2023;73(1):17–48. doi:10.3322/caac.21763
4. Xiang Z, Huang Y, Ma J, et al. Temporal trends of incidence, mortality, and survival of liver cancer during 2011-2020 in Fujian Province, Southeast China. *Arch Public Health*. 2024;82(1):233. doi:10.1186/s13690-024-01462-7
5. Han B, Zheng R, Zeng H, et al. Cancer incidence and mortality in China, 2022. *J Natl Cancer Cent*. 2024;4(1):47–53. doi:10.1016/j.jncc.2024.01.006
6. McGlynn KA, Petrick JL, El-Serag HB. Epidemiology of Hepatocellular Carcinoma. *Hepatology*. 2021;73(Suppl 1):4–13. doi:10.1002/hep.31288
7. Choi S, Kim BK, Yon DK, et al. Global burden of primary liver cancer and its association with underlying aetiologies, sociodemographic status, and sex differences from 1990-2019: a DALY-based analysis of the Global Burden of Disease 2019 study. *Clin Mol Hepatol*. 2023;29(2):433–452. doi:10.3350/cmh.2022.0316
8. Hwang SY, Danpanichkul P, Agopian V, et al. Hepatocellular carcinoma: updates on epidemiology, surveillance, diagnosis and treatment. *Clin Mol Hepatol*. 2025;31(Suppl):S228–S254. doi:10.3350/cmh.2024.0824
9. Kanwal F, Kramer JR, Mapakshi S, et al. Risk of Hepatocellular Cancer in Patients With Non-Alcoholic Fatty Liver Disease. *Gastroenterology*. 2018;155(6):1828–1837.e2. doi:10.1053/j.gastro.2018.08.024
10. Chidambaranathan-Reghupaty S, Fisher PB, Sarkar D. Hepatocellular carcinoma (HCC): epidemiology, etiology and molecular classification. *Adv Cancer Res*. 2021;149:1–61. doi:10.1016/bs.acr.2020.10.001
11. Zhen WC, Sun J, Bai XT, et al. Trends of alkaline phosphatase to prealbumin ratio in patients with hepatitis B linked to hepatocellular carcinoma development. *World J Gastroenterol*. 2025;31(2):99349. doi:10.3748/wjg.v31.i2.99349
12. Llovet JM, Kelley RK, Villanueva A, et al. Hepatocellular carcinoma [published correction appears in Nat Rev Dis Primers. *Nat Rev Dis Primers*. 2021;7(1):6. doi:10.1038/s41572-020-00240-3
13. Luo X, He X, Zhang X, et al. Hepatocellular carcinoma: signaling pathways, targeted therapy, and immunotherapy. *MedComm*. 2024;5(2):e474. doi:10.1002/mco2.474
14. Shah P, Shende P. Biomacromolecule-Functionalized Nanoparticle-Based Conjugates for Potentiation of Anticancer Therapy. *Curr Cancer Drug Targets*. 2022;22(1):31–48. doi:10.2174/1568009621666211206102942
15. Li K, Xiao K, Zhu S, Wang Y, Wang W. Chinese Herbal Medicine for Primary Liver Cancer Therapy: perspectives and Challenges. *Front Pharmacol*. 2022;13:889799. doi:10.3389/fphar.2022.889799
16. Lv M, Liang Q, He X, et al. Hypoglycemic effects of dendrobium officinale leaves. *Front Pharmacol*. 2023;14:1163028. doi:10.3389/fphar.2023.1163028
17. Zhang P, Zhang X, Zhu X, Hua Y. Chemical Constituents, Bioactivities, and Pharmacological Mechanisms of *Dendrobium officinale*: a Review of the Past Decade. *J Agric Food Chem*. 2023;71(41):14870–14889. doi:10.1021/acs.jafc.3c04154
18. He Y, Li L, Chang H, et al. Research progress on extraction, purification, structure and biological activity of *Dendrobium officinale* polysaccharides. *Front Nutr*. 2022;9:965073. doi:10.3389/fnut.2022.965073
19. Luo Y, Liu G, Hou P. Synergism Effect of Dendrobine on Cisplatin in Treatment of H1299 by Modulating the Balance of Treg/Th17. *Anticancer Agents Med Chem*. 2023;23(1):105–112. doi:10.2174/1871520622666220520093837
20. Wang Y, Chu F, Lin J, et al. Erianin, the main active ingredient of Dendrobium chrysotoxum Lindl, inhibits precancerous lesions of gastric cancer (PLGC) through suppression of the HRAS-PI3K-AKT signaling pathway as revealed by network pharmacology and in vitro experimental verification. *J Ethnopharmacol*. 2021;279:114399. doi:10.1016/j.jep.2021.114399
21. Wang HY, Ge JC, Zhang FY, et al. Dendrobium officinale polysaccharide promotes M1 polarization of TAMs to inhibit tumor growth by targeting TLR2. *Carbohydr Polym*. 2022;292:119683. doi:10.1016/j.carbpol.2022.119683
22. Hong J, Xie Z, Yang F, et al. Erianin suppresses proliferation and migration of cancer cells in a pyruvate carboxylase-dependent manner. *Fitoterapia*. 2022;157:105136. doi:10.1016/j.fitote.2022.105136
23. Yang L, Hu Y, Zhou G, Chen Q, Song Z. Erianin suppresses hepatocellular carcinoma cells through down-regulation of PI3K/AKT, p38 and ERK MAPK signaling pathways. *Biosci Rep*. 2020;40(7):BSR20193137. doi:10.1042/BSR20193137
24. Xing S, Zhang X, Ke H, Lin J, Huang Y, Wei G. Physicochemical properties of polysaccharides from Dendrobium officinale by fractional precipitation and their preliminary antioxidant and anti-HepG2 cells activities in vitro. *Chem Cent J*. 2018;12(1):100. doi:10.1186/s13065-018-0468-4
25. Zhao R, Luo J, Kim chung S, Xu B. Anti-depression molecular mechanism elucidation of the phytochemicals in edible flower of *Hemerocallis citrina* Baroni. *Food Sci Nutr*. 2024;12(12):10164–10180. doi:10.1002/fsn3.4446
26. Chintaluri PG, Ganapathy Vilasam Sreekala A, Gupta KK, Sivadasan A, Nathan VK. Network pharmacological evaluation of *Cressa cretica* L.- an integrated approach of modern and ancient pharmacology. *J Biomol Struct Dyn*. 2025;4:1–16. doi:10.1080/07391102.2025.2472403
27. Fang S, Su H, Liu J, et al. Network pharmacology and molecular docking to explore the potential mechanism of chlorogenic acid in septic acute liver injury and experimental validation of TLR4/NF-κB pathway in vivo. *Naunyn Schmiedebergs Arch Pharmacol*. 2025;398(6):7331–7342. doi:10.1007/s00210-024-03712-5
28. Pinzi L, Rastelli G. Molecular Docking: shifting Paradigms in Drug Discovery. *Int J Mol Sci*. 2019;20(18):4331. doi:10.3390/ijms20184331

29. Li H, Guo L, Ding X, et al. Molecular Networking, Network Pharmacology, and Molecular Docking Approaches Employed to Investigate the Changes in Ephedrae Herba before and after Honey-Processing. *Molecules*. 2022;27(13):4057. doi:10.3390/molecules27134057
30. Li W, Jiao R, Luo S, Liu Z, Song J, Chen Z. Mechanism of action of Coptidis Rhizome in treating periodontitis based on network pharmacology and in vitro validation. *BMC Oral Health*. 2024;24(1):530. doi:10.1186/s12903-024-04311-9
31. Yu S, Gao W, Zeng P, et al. Exploring the effect of Gupi Xiaoji Prescription on hepatitis B virus-related liver cancer through network pharmacology and in vitro experiments. *Biomed Pharmacother*. 2021;139:111612. doi:10.1016/j.biopha.2021.111612
32. Chen K, Jin C, Cheng YY, Zhang QX, Li XX, Zhang L. Molecular mechanism of Spatholobi Caulis in treatment of lung cancer based on network pharmacology and molecular docking. *Zhongguo Zhong Yao Za Zhi*. 2021;46(4):837–844. doi:10.19540/j.cnki.cjcmm.20201118.401
33. Sung H, Ferlay J, Siegel RL, et al. Global Cancer Statistics 2020: GLOBOCAN Estimates of Incidence and Mortality Worldwide for 36 Cancers in 185 Countries. *CA Cancer J Clin*. 2021;71(3):209–249. doi:10.3322/caac.21660
34. Guo Q, Zhu X, Beeraka NM, et al. Projected epidemiological trends and burden of liver cancer by 2040 based on GBD, CI5plus, and WHO data. *Sci Rep*. 2024;14(1):28131. doi:10.1038/s41598-024-77658-2
35. Zhou J, Sun H, Wang Z, et al. Guidelines for the Diagnosis and Treatment of Primary Liver Cancer (2022 Edition). *Liver Cancer*. 2023;12(5):405–444. doi:10.1159/000530495
36. Shen J, Wen J, Li C, et al. The prognostic value of microvascular invasion in early-intermediate stage hepatocelluar carcinoma: a propensity score matching analysis. *BMC Cancer*. 2018;18(1):278. doi:10.1186/s12885-018-4196-x
37. Rizzo A, Ricci AD. Challenges and Future Trends of Hepatocellular Carcinoma Immunotherapy. *Int J Mol Sci*. 2022;23(19):11363. doi:10.3390/ijms231911363
38. Rizzo A, Ricci AD, Brandi G. Trans-Arterial Chemoembolization Plus Systemic Treatments for Hepatocellular Carcinoma: an Update. *J Pers Med*. 2022;12(11):1788. doi:10.3390/jpm12111788
39. Shaikh S, Kunchala D, Patel M, Velecha D, Prajapati S, Gupta R. Reverse Vaccinology and Immunoinformatics Strategy to Screen Oncogenic Proteins and Development of a Multiepitope Peptide Vaccine Targeting Protein Kinases against Oral Cancer: an in-silico Study. *Asian Pac J Cancer Prev*. 2024;25(11):4067–4080. doi:10.31557/APJCP.2024.25.11.4067
40. Zhang J, Li C, Li W, et al. Mechanism of luteolin against non-small-cell lung cancer: a study based on network pharmacology, molecular docking, molecular dynamics simulation, and *in vitro* experiments. *Front Oncol*. 2024;14:1471109. doi:10.3389/fonc.2024.1471109
41. Noorolyai S, Shajari N, Baghbani E, Sadreddini S, Baradaran B. The relation between PI3K/AKT signalling pathway and cancer. *Gene*. 2019;698:120–128. doi:10.1016/j.gene.2019.02.076
42. Rogel A, Willoughby JE, Buchan SL, Leonard HJ, Thirdborough SM, Al-Shamkhani A. Akt signaling is critical for memory $CD8^+$ T-cell development and tumor immune surveillance. *Proc Natl Acad Sci U S A*. 2017;114(7):E1178–E1187. doi:10.1073/pnas.1611299114
43. Zhang Q, Dai HH, Dong HY, Sun CT, Yang Z, Han JQ. EGFR mutations and clinical outcomes of chemotherapy for advanced non-small cell lung cancer: a meta-analysis. *Lung Cancer*. 2014;85(3):339–345. doi:10.1016/j.lungcan.2014.06.011
44. Bruix J, Sherman M, Llovet JM, et al. Clinical management of hepatocellular carcinoma. Conclusions of the Barcelona-2000 EASL conference. European Association for the Study of the Liver. *J Hepatol*. 2001;35(3):421–430. doi:10.1016/s0168-8278(01)00130-1
45. Wang X, Liu X, Yang Y, Yang D. Cyclin D1 mediated by the nuclear translocation of nuclear factor kappa B exerts an oncogenic role in lung cancer. *Bioengineered*. 2022;13(3):6866–6879. doi:10.1080/21655979.2022.2043099
46. Zhang H, He C, Guo X, et al. DDX39B contributes to the proliferation of colorectal cancer through direct binding to CDK6/CCND1. *Cell Death Discov*. 2022;8(1):30. doi:10.1038/s41420-022-00827-7
47. Huang T, Jiang K, Li L, Li G, Cao Y, Huang X. Hsa_circ_0000423 promotes colorectal cancer EMT and immune escape by competitive adsorption of miR-369-3p mediating CCND1 expression. *Discov Oncol*. 2024;15(1):634. doi:10.1007/s12672-024-01501-3
48. Xiong Y, Connolly T, Futcher B, Beach D. Human D-type cyclin. *Cell*. 1991;65(4):691–699. doi:10.1016/0092-8674(91)90100-d
49. Yan W, Cheng L, Zhang D. Ultrasound-Targeted Microbubble Destruction Mediated si-CyclinD1 Inhibits the Development of Hepatocellular Carcinoma via Suppression of PI3K/AKT Signaling Pathway. *Cancer Manag Res*. 2020;12:10829–10839. doi:10.2147/CMAR.S263590
50. Dong T, Zhang Y, Chen Y, et al. FOXO1 inhibits the invasion and metastasis of hepatocellular carcinoma by reversing ZEB2-induced epithelial-mesenchymal transition. *Oncotarget*. 2017;8(1):1703–1713. doi:10.18632/oncotarget.13786
51. Luo Y, Guo C, Ling C, et al. Pine pollen reverses the function of hepatocellular carcinoma by inhibiting α-Enolase mediated PI3K/AKT signaling pathway. *PLoS One*. 2024;19(11):e0312434. doi:10.1371/journal.pone.0312434